KURENAI

Kyoto University Research Information Repository

KYOTO UNIVERSITY

Title	Structures and magnetism of two types of c(2x2)-Mn/Pd(001) surface alloys
Author(s)	Tsuboi, N; Okuyama, H; Aruga, T
Citation	PHYSICAL REVIEW B (2005), 71(19)
Issue Date	2005-05
URL	http://hdl.handle.net/2433/50056
Right	Copyright 2005 American Physical Society
Type	Journal Article
Textversion	publisher

Kyoto University

Structures and magnetism of two types of $c(2\times2)$-Mn/Pd(001) surface alloys

N. Tsuboi, H. Okuyama, and T. Aruga*

Department of Chemistry, Graduate School of Science, Kyoto University, Kyoto 606-8502, Japan

(Received 5 December 2004; revised manuscript received 20 January 2005; published 24 May 2005)

Mn/Pd(001) surface alloy was investigated by a tensor low-energy electron diffraction (LEED) analysis. After deposition of Mn on Pd(001) at room temperature, the surface was annealed at 570–620 K, which produced two types of $c(2\times2)$ surface alloys, according to the Mn coverage. At a low-Mn coverage, we obtained a Pd-capped $c(2\times2)$ surface, in which the first layer was composed of a (1×1)-Pd layer, and the second layer was a $c(2\times2)$-MnPd mixed layer [α-$c(2\times2)$]. The deposition of greater amounts of Mn followed by annealing resulted in another $c(2\times2)$ surface, in which Mn atoms existed in the substitutional sites of the first and third layers [β-$c(2\times2)$]. The first layer consisted of a $c(2\times2)$-MnPd mixed layer, the second layer was a (1×1)-Pd layer, and the third layer was another $c(2\times2)$-MnPd mixed layer. The structure of the β-$c(2\times2)$ surface qualitatively agreed with the one previously investigated by LEED. These two types of surface alloys, α-$c(2\times2)$ and β-$c(2\times2)$, may be considered as being precursors to the formation of the bulk $MnPd_3$ alloy. We also investigated the magnetic properties of the α-$c(2\times2)$ and β-$c(2\times2)$ surfaces by using surface magneto-optic Kerr effect (MOKE) and self-consistent, total-energy calculations. The MOKE measurements for both surface alloys show no hysterisis loop, even at 10 K. The total-energy calculation shows that Mn atoms have a local-spin moment of 3.9–4.1 μ_B and that they are antiferromagnetically ordered in the ground state.

I. INTRODUCTION

The magnetism of surfaces has attracted wide attention, because the low-dimensionality of the surfaces induces the changing of magnetic properties. Manganese is an interesting element that exists in four modifications with different magnetic properties.[1,2] It is known that Mn provides epitaxial growth or formation of ordered surface alloys on appropriate substrates.[3–10] Long-range magnetic order was observed on the Mn/Ni(001) (Ref. 10) and Mn/Ag(001) (Ref. 9) surfaces. On the Ni(001)-$c(2\times2)$-Mn surface with 0.5-monolayer (ML) Mn in the first-layer substitutional sites, Mn atoms were found to be ferromagnetically ordered and relaxed outwards by 0.25 Å.[6] The stability of the alloy has been theoretically predicted to be due to the magnetic energy gain of the Mn atoms.[5] On the Ag(001) surface the Mn atoms in an ideal monolayer were suggested to have an antiferromagnetic order below 200 K, based on the low-energy electron-diffraction (LEED) observation of a c-(2×2) antiferromagnetic to $p(1\times1)$ paramagnetic phase transition. The Mn—Ag interlayer distance was investigated by LEED analysis at 100 K. It yielded $d_{12}=2.00$ Å, which is much larger than the 1.85 Å expected from the simple addition of atomic radii in elemental α-Mn and fcc Ag. Such interlayer expansions were considered as evidence of a strong reduction in the Mn 3d contribution to cohesion, due to a development of high local magnetic moments of Mn atoms.

Mn/Pd(001) was also expected to have a large magnetic moment.[12–14] In a previous study, it was reported that the room-temperature deposition of Mn on Pd(001) yielded a diffuse $c(2\times2)$ LEED pattern and that annealing this surface improved the ordering.[3,15] A preliminary structure analysis by LEED was also performed. It was suggested that, on the as-deposited surface, a mixed Mn-Pd surface layer was formed with the Mn sublayer 0.2 Å above the Pd sublayer.[3]

The annealed surface was also analyzed by using a semi-infinite Pd$_3$Mn(001) surface as a model. The analysis showed that the surface was terminated with a $c(2\times2)$-MnPd mixed layer and that the Mn sublattice on the topmost layer was then *below* the Pd sublattice by 0.2 Å. The total-energy calculation suggested that the Mn atoms of the annealed $c(2\times2)$ surface strongly tended to spin polarize with spin moments between 3.8 and 4.3 μ_B.[16] The energy difference between the ferromagnetic and antiferromagnetic states was close. It, therefore, was suggested that the system might have been in a spin-disordered, paramagnetic state.

In this paper we report that there is another stable phase which also has a AuCu$_3$-type structure, but the top layer is a (1×1)-Pd layer. The new surface is obtained by annealing the surface with a lower Mn coverage. We analyze the structure of this new phase and also refine the structure of the previously studied phase by LEED. We also present the results of magnetic measurement by using the magneto-optic Kerr effect (MOKE) technique and total-energy calculations.

II. EXPERIMENTAL AND THEORETICAL METHODS

Our experiments were carried out in an ultrahigh vacuum chamber with a base pressure of about 3×10^{-10} Torr, which is equipped with standard four-gird LEED optics and a facility for MOKE measurement. The Pd(001) sample was cleaned by cycles of Ar$^+$ sputtering and annealing. In addition, several times of oxygen treatment were done to remove residual carbon. Mn was evaporated from an Al$_2$O$_3$ crucible. The evaporation rate was calibrated by monitoring Pd Auger peak intensities of the unheated surface which showed linear decrease. During the deposition, the sample temperature was held at room temperature and the pressure less than 8×10^{-10} Torr.

In the LEED experiment, the intensity against primary-energy (I-V) curves was recorded with a normal incident beam in the energy range of 40–460 eV in steps of 2 eV. LEED simulations based on the dynamical theory were carried out using the Barbieri-Van Hove SYMMETRIZED AUTOMATED TENSOR LEED (SATLEED) package.[17] This program is based primarily on conventional LEED theory,[18] which simulates fully and dynamically the multiple scattering of electrons by individual atoms of a semi-infinite crystal by assuming spherically symmetrical potentials surrounded by regions of constant potential. Electron scattering by the potential is described by partial-wave phase shifts. The tensor LEED approximation is based on the assumption that, given a correct diffraction intensity from a reference structure, the change in the intensity resulting from small displacements of the atoms away from this reference structure can be evaluated by a perturbation expansion in terms of those small displacements. Ten phase shifts calculated with the Barbieri-Van Hove phase-shift program were used to describe the atomic scattering of Pd and Mn atoms. The agreement between the calculated and experimental I-V curves was measured using the Pendry R factor (R_P).[19] The Pendry R factor treats all peaks with equal weight and is chiefly sensitive to peak positions that are directly related to the geometry. It does not weight the peaks in proportion to their height, because intensities of the peaks are less well accounted for since they are influenced by thermal vibrations, atomic scattering effects, and many other effects. The imaginary part of the inner potential was set at -5 eV, and the real part was fitted during the optimized process.

The magnetic properties were detected by the *in situ* MOKE technique using a He-Ne laser ($\lambda = 632.8$ nm). A maximum applied field was 1200 and 80 Oe, respectively, for longitudinal and polar configuration.

The self-consistent total-energy calculations were performed by using WIEN2k code.[20,21] The calculations are based on the scalar-relativistic full-potential (FP) augmented plane wave+local orbitals (APW+lo) method.[22,23] The generalized-gradient approximation[24] was used for the exchange and correlation potential. The RK_{max} parameter, in which R denotes the minimum atomic sphere for the APW+lo basis and K_{max} the cut-off wave vector for the plane waves, determined the accuracy of the calculation with respect to the basis-set size. In the present work, the atomic sphere for Mn and Pd was set at 2.3 and 2.4 a.u., respectively. The structure optimization was done successively with increasing RK_{max} from 7.0 to 9.0. Optimized atomic positions were well converged above $RK_{max} = 8.0$. It was found that $RK_{max} = 9.0$, which corresponds to the basis-set size of 4000–7000, gives the convergence within ~ 5 meV for the total-energy difference between the values for two different structures. In most of the calculations, 15 (10) k points in irreducible Brillouin-zone wedges were used for $c(2 \times 2)$ $[p(2 \times 2)]$ surfaces, which corresponded to the 10×10 (8×8) meshes in the whole surface Brillouin zone. For some structures, calculations with 21 and 28 k points were performed to check the convergence. For the total-energy differences given below, the convergence with respect to the number of k points was estimated to be ~ 10 meV. The

surfaces were modeled by periodic slabs that consisted of five layers of central Pd layers and bilayer or trilayer surface alloys on both sides. The lateral lattice constants were adjusted for the optimized lattice constant for fcc Pd, which was 1.5% larger than the experimental value. The comparisons with the experimental structural parameters were made by rescaling the optimized structures to the bulk-Pd-lattice constant.

III. RESULTS

The Mn deposition on the Pd(001) surface at 300 K gave rise to a diffuse $c(2 \times 2)$ LEED pattern. Upon annealing at 570–620 K a sharp $c(2 \times 2)$ LEED pattern developed. We found that there are two types of the ordered surfaces, by plotting the intensities of the $(\frac{1}{2}, \frac{1}{2})$, $(1,0)$ and $(\frac{3}{2}, \frac{1}{2})$ spots of the 570 K annealed surfaces as a function of the Mn deposition time. The intensities of the half-order spots showed the first maxima at 11 min, indicating the formation of the ordered surface $[\alpha\text{-}c(2 \times 2)]$. Further Mn deposition decreased the intensities, but again gave rise to the second maxima at 17 min, which suggests the other ordered structure $[\beta\text{-}c(2 \times 2)]$. The LEED I-V curves of fractional spots measured for these two surfaces had completely different shapes. Upon further deposition, the LEED spots gradually became diffuse, keeping the same I-V features as those of the $\beta\text{-}c(2 \times 2)$ surface. The I-V curves from the $\beta\text{-}c(2 \times 2)$ surface agreed well with those from the $c(2 \times 2)$ surface previously studied.[3] According to the previous scanning tunneling microscopy (STM) study[15] a flat $\beta\text{-}c(2 \times 2)$ structure covering the whole surface was found for the Mn coverage of 0.7–1.0 ML. This suggests that the $\alpha\text{-}c(2 \times 2)$ structure was formed for the Mn coverage of 0.45–0.65 ML. Between the coverages for the formation of $\alpha\text{-}c(2 \times 2)$ and $\beta\text{-}c(2 \times 2)$, the profile of each LEED spot gradually changed from that of $\alpha\text{-}c(2 \times 2)$ to $\beta\text{-}c(2 \times 2)$, as Mn coverage increased. This indicated that the surface was covered with both types of surface alloys, except at their ideal Mn coverages. The STM study[15] for coverages of about 0.3 and 0.7 ML of Mn on Pd(100) showed that, after annealing, two-dimensional islands were created on the Pd(100) terraces. Our LEED analysis implied that at 0.3 ML the $\alpha\text{-}c(2 \times 2)$ islands were formed on the bare Pd(100) terraces, and at 0.7 ML the $\beta\text{-}c(2 \times 2)$ islands were formed on the $\alpha\text{-}c(2 \times 2)$ terraces. It would be difficult to distinguish the $\alpha\text{-}c(2 \times 2)$ domains and bare Pd(100) by using STM, because the top layer is composed of (1×1)-Pd.

We measured LEED I-V curves at the sample temperature of 80 K. On both surfaces we employed seven independent beams, $(\frac{1}{2}, \frac{1}{2})$, $(1,0)$, $(1,1)$, $(\frac{3}{2}, \frac{1}{2})$, $(2,0)$, $(\frac{3}{2}, \frac{3}{2})$, and $(2,1)$. The total-energy ranges were 2240 and 2278 eV, respectively, for the $\alpha\text{-}c(2 \times 2)$ and $\beta\text{-}c(2 \times 2)$ surfaces. Six models consisting of the Mn coverages of 0.5 and 1.0 ML were tested (Table I). In the screening survey of the models with 0.5-ML Mn (CP, PC, HP), the relaxations in the outermost two interlayer spacings and the buckling amplitude of a $c(2 \times 2)$-PdMn mixed layer were allowed, and of the models with

TABLE I. $c(2\times2)$ models of the α-$c(2\times2)$ and β-$c(2\times2)$ surfaces and the R_P values in the screening analysis. The R_P values in parentheses are obtained in the refinement analysis.

Model	First layer	Second layer	Third layer	R_P—α-$c(2\times2)$ surface	R_P—β-$c(2\times2)$ surface
CP	$c(2\times2)$-PdMn	$p(1\times1)$-Pd		0.54	0.29(0.27)
PC	$p(1\times1)$-Pd	$c(2\times2)$-PdMn		0.27(0.20)	0.57
HP	$c(2\times2)$-Mn-hollow	$p(1\times1)$-Pd		0.66	0.70
CPC	$c(2\times2)$-PdMn	$p(1\times1)$-Pd	[a]$c(2\times2)$-PdMn[1]	0.55	0.25(0.23)
CPC′	$c(2\times2)$-PdMn	$p(1\times1)$-Pd	[a]$c(2\times2)$-PdMn[2]	0.63	0.48
CCP	$c(2\times2)$-PdMn	$c(2\times2)$-PdMn	$p(1\times1)$-Pd	0.54	0.48

[a]The third layer Mn exists just below the first layer [1]Mn or [1]Pd.

1.0-ML Mn (CPC, CPC′, CCP), we allowed the relaxation of the outermost three interlayer spacings and the buckling amplitudes of the $c(2\times2)$-PdMn mixed layers. The R_P values are listed in Table I.

The LEED calculations of the α-$c(2\times2)$ structure demonstrated that the (1×1)-Pd/$c(2\times2)$-PdMn/(1×1)-Pd structure [PC, see Fig. 1(a)] exhibited the best agreement with experiment, $R_P=0.27$. The variance[19] was 0.03. The other models resulted in the R_P values between 0.41 and 0.69 and were excluded. We further refined the PC structure by the optimization of the relaxations of the outermost three interlayer spacings and the Debye temperatures. The resulting R_P value was 0.20. Fig. 2(a) shows the comparison of the experimental and calculated LEED I-V curves for the PC structure. The agreement between experiment and theory is good. The optimized values for the structural parameters [the interlayer distances, d_{12}, d_{23}, d_{34} and the intralayer buckling in the second layer δ, as defined in Fig. 1(a)] are listed in Table II. We found that the first interlayer distance, $d_{12}=2.02$ Å was expanded by 3.8% from that in bulk Pd (1.945 Å). In the buckled second layer the Mn sublayer was located slightly above the Pd sublayer by 0.03 Å. The optimized Debye temperatures were 140, 200, and 210 K, respectively, for Pd in the first layer, Pd in the second layer, and Mn in the second layer. The Debye temperatures for Pd in the third and deeper layers were kept at 280 K. The PC structure was regarded as one termination of the MnPd$_3$ bulk alloy, which has a AuCu$_3$-type cubic structure with Pd and MnPd layers stacked alternatively along the [001] direction.

We next analyzed the β-$c(2\times2)$ surface by examining the same models. The CP and CPC models gave rise to R_P of 0.29 and 0.25, respectively, while the other models resulted in R_P larger than 0.48. The CPC model was considered as the other termination of the MnPd$_3$ bulk alloy, with the top and the third layer being $c(2\times2)$-MnPd mixed layers, and a (1×1)-Pd second layer [Fig. 1(b)]. The CP model was similar to the CPC model, except that Mn atoms existed only in the substitutional sites of the first layer. We further optimized these two structures, taking account of the Debye temperatures, and for the CPC model, the relaxation of the third layer. The optimization of the CPC model yielded $R_P=0.23$ and the variance of 0.03, and the CP model yielded $R_P=0.27$. The result indicated that the β-$c(2\times2)$ surface was composed of the CPC model. This model contained 1.0-ML Mn atoms, which was in accordance with the fact that β-$c(2\times2)$ was formed at initial Mn coverages higher than that for α-$c(2\times2)$. In Fig. 2(b), the experimental I-V curves are compared with those for the CPC model. The agreement between experiment and theory is good. The optimized Debye temperatures are 220 K and 230 K for Pd in the first layer and Mn in the first and third layers.
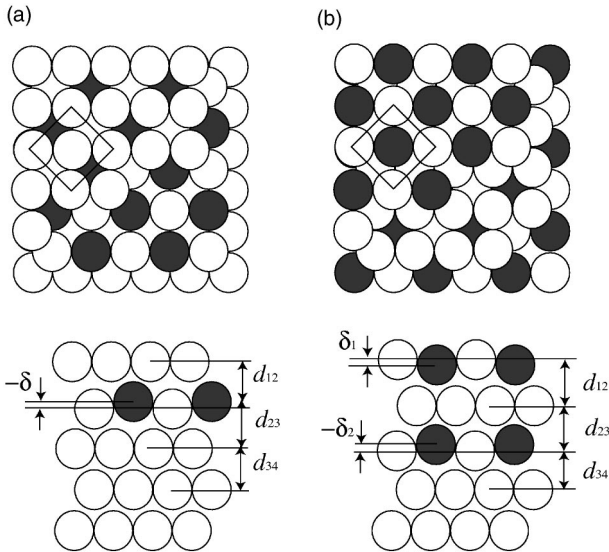

FIG. 1. Models of the Pd(001)-$c(2\times2)$-Mn surface alloys. Top and side views of the PC structure (a) and the CPC structure (b). The white spheres are Pd atoms, and the black spheres are Mn atoms.

TABLE II. Optimized parameters of the best-fit α-$c(2\times2)$ and β-$c(2\times2)$ structures, and that of the previous analyzed β-$c(2\times2)$ structure.

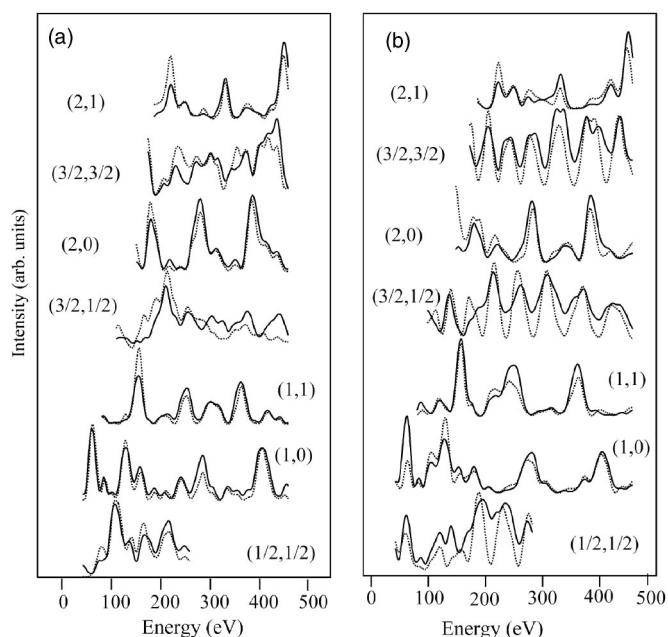| Parameters (Å)	α-$c(2\times2)$	β-$c(2\times2)$	β-$c(2\times2)$ (Ref. 3)
d_{12}	2.02 ± 0.02	1.98 ± 0.03	1.95
d_{23}	1.93 ± 0.02	1.97 ± 0.02	1.94
d_{34}	1.96 ± 0.02	1.95 ± 0.02	
δ	-0.03 ± 0.02		
δ_1		0.04 ± 0.03	0.2
δ_2		0.04 ± 0.02	

FIG. 2. Comparison between experimental (solid) and calculated (dotted) I-V curves for (a) the α-$c(2\times2)$ surface and (b) the β-$c(2\times2)$ surface.
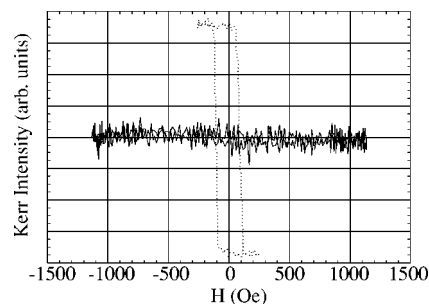

FIG. 3. Longitudinal Kerr signal of an α-$c(2\times2)$ surface (solid). There is no magnetic response. The dotted line is a hysteresis loop of Ni/Pd(001), measured at 80 K for reference.

IV. TOTAL-ENERGY CALCULATIONS

We estimated the structural stability by carrying out a self-consistent total-energy calculation. In a previous investigation, a total-energy calculation by the relativistic Green function Korringa-Kohn-Rostocker (GFKKR) method was performed for several PdMn surface alloys with 1-ML Mn atoms.[16] The calculation indicated that a Pd-terminated $AuCu_3$ structure (PCPC) is energetically more stable than the PdMn-terminated $AuCu_3$ structure (CPC). This contradicted the LEED results that the Mn/Pd(001) surface alloy at the amount of 1-ML Mn atoms consists of a PdMn-teminated surface. They conjectured that the system was not able to reach PCPC state at the used annealing temperature due to kinetic constraints. We performed extended calculations for several PdMn surface alloys with 0.5-ML Mn atoms. Mn atoms were located at hollow sites (HP), at substitutional sites in the first layer (CP), and at substitutional sites in the second layer (PC). The total-energy differences for these structures, both spin-polarized (SP) and spin-unpolarized (UP) are summarized in Table III. The data indicate that the spin-polarized PC surface is the most stable one. This structure is comparable to the α-$c(2\times2)$ model that we obtained by the LEED analysis.

We also calculated the total energies of spin-polarized (SP) and spin-unpolarized (UP) configurations for the α-$c(2\times2)$ and β-$c(2\times2)$ surface alloys in order to investigate the detailed magnetic properties. Table IV shows the optimized structural parameters and total energies of spin-polarized (SP) and spin-unpolarized (UP) surfaces. We can see the close relationship between the atomic and the magnetic structures. Compared to the spin-polarized surfaces, the unpolarized surfaces have distinctly shorter interlayer dis-

This structure was already investigated by LEED.[3] In Table II, the optimized parameters for the best-fit β-$c(2\times2)$ structure of our analysis and previous LEED analyses are given. Comparing these two data we find that the buckling of the first layer of our model, $\delta_1 = 0.04$ Å, is much smaller than that of the previous result, $\delta_1 = 0.2$ Å. There is only a small difference between these two sets of I-V curves, so we believe that the discrepancy is due to the analysis procedure, including the number of the parameters employed, the total data quantity used, and especially the model used. The previous model was based on the assumption that the annealing would favor the formation of a bulk alloy extending four or more layers into the Pd substrate.[3] The first and second interlayer distances, $d_{12} = 1.98$ Å and $d_{23} = 1.97$ Å, are slightly expanded from the bulk Pd spacing of 1.945 Å. The third layer is slightly buckled with the Mn atoms displaced outwards by 0.04 Å.

Next we studied the magnetic properties using the MOKE technique. The measurement was made at 10 K, and just before the measurement we flashed the sample up to 570 K to reduce the influence of the gas adsorption. The magnetic structure of the bulk $MnPd_3$ alloy had been reported to have two configurations depending on its structure, the cubic $AuCu_3$ type and the tetragonal $ZrAl_3$ type. The latter structure was understood as $AuCu_3$-type structure modulated by antiphase boundaries in every two unit cells along the c axis. The $ZrAl_3$-type one had a collinear, layered antiferromagnetic order with the magnetic moments pointing mainly along the a axis.[26,27] If we considered the α- and β-$c(2\times2)$ surface alloys as terminations of the $MnPd_3$ bulk alloy of the $ZrAl_3$ type, the magnetic moments in the (001) face could have been expected to have ferromagnetic order. However, as shown in Fig. 3, no hysteresis loop was observed on the α-$c(2\times2)$ or β-$c(2\times2)$ surface alloys, even though the temperature was as low as 10 K.

TABLE III. Difference in total energies of the surfaces with 0.5-ML Mn per $c(2\times2)$ unit, in eV, for spin-polarized (SP) and spin-unpolarized (UP) conditions.

	SP	UP
HP	1.00	4.77
CP	0.32	2.50
PC	0.00	1.66

TABLE IV. Structural parameters optimized by FP-APW+lo for spin-polarized (SP) and spin-unpolarized (UP) surfaces of α-$c(2\times2)$ and β-$c(2\times2)$.

Parameters (Å)	α-$c(2\times2)$		β-$c(2\times2)$	
	SP	UP	SP	UP
d_{12}	1.81	1.77	1.97	1.86
d_{23}	1.90	1.78	1.94	1.85
d_{34}	1.93	1.95	1.92	1.81
δ	0.02	0.01		
δ_1			−0.17	−0.2
δ_2			0.00	−0.12
total energy [eV/$c(2\times2)$]	0.00	+1.66	0.00	+4.09

tances. This indicates that the magnetic moments of Mn atoms expand the lattice. The distances of the spin-polarized surfaces fairly reproduce the experimental values. The total energy suggests that the spin-polarized surfaces are more stable than the unpolarized surfaces by 1.66 and 4.09 eV, respectively, for the α-$c(2\times2)$ and β-$c(2\times2)$ surfaces. We obtained the magnetic moment of 3.94 μ_B for the Mn atoms on the α-$c(2\times2)$ surface and 4.13 and 3.95 μ_B for the first and third layer Mn atoms on β-$c(2\times2)$ surface. These values are similar to the value of the Mn atoms in the MnPd$_3$ bulk alloy, ~4 μ_B.[26,27] We also performed calculations for the ferromagnetic (FM) and antiferromagnetic (AFM) alignments of the Mn moments. On each surface an AFM configuration had a lower energy than a FM configuration. The differences of the total energies between the FM and AFM states were 3 and 29 meV, respectively, for α-$c(2\times2)$ and β-$c(2\times2)$.

V. DISCUSSION

Two types of surface alloys were found, according to the Mn coverage. They may be the formation of the bulk MnPd$_3$ alloy of the AuCu$_3$ type. Three outermost layers were similar to the termination of MnPd$_3$. The interlayer distances between the first and third Pd layers were 3.95 and 3.96 Å, respectively, for the α-$c(2\times2)$ and β-$c(2\times2)$ surfaces. They should be compared with that of the MnPd$_3$ of 3.90 Å.[25]

Ti/Pd(001)-$c(2\times2)$-H and V/Pd(001)-$c(2\times2)$ surface alloys had the same structural type as the α-$c(2\times2)$-Mn/Pd(001) surface.[28,29] Comparing the intralayer distances between the first and third Pd layers of these three surface alloys, we found that the α-$c(2\times2)$-Mn surface had an especially long distance, $d_{Ti}=3.78$ Å, $d_V=3.75$ Å, and $d_{Mn}=3.95$ Å, where d_A denotes the distance between the first and third Pd layers of the A/Pd(001) surface alloy. The atomic radius of Mn took various values from 1.3 to 1.4 Å depending on its structure, and those of Ti and V were 1.45 Å and 1.31 Å, respectively.[1,5,11] These values suggest that the discrepancies between atomic radii are not the origins of the structural properties. The lattice expansion can be explained by taking account of the largest magnetic moment

of Mn.[12–14] In general, a high-spin ground state is thought to cause a lattice expansion due to the strong reduction in the contribution of the magnetic elements to cohesion.[30]

The MOKE measurements showed no ferromagnetic configurations at 10 K. This indicates that the surface alloys have different magnetic orders from the bulk MnPd$_3$ alloy of the ZrAl$_3$ type. The total-energy calculation suggests that Mn atoms possess atomiclike large magnetic moments, ~4 μ_B, and the AFM state is the magnetic ground state for both surface alloys. However, the differences of the total energies between AFM and FM states are small. In particular, they are almost degenerated for α-$c(2\times2)$. The small energy differences indicate that there is competition on the surface magnetic configuration between the AFM and FM states. We roughly estimated the critical temperature for the AFM phase by adopting the Heisenberg model. The exchange integral J was calculated from the difference of the total energies between the FM and AFM configurations to be 0.11 and 0.39 meV for the α-$c(2\times2)$ and β-$c(2\times2)$ surfaces, respectively. By using the mean-field approximation (MFA), the critical temperature was estimated to be 14 K for α-$c(2\times2)$ and 66 K for β-$c(2\times2)$. Considering that the estimation using MFA generally overestimates the critical temperature by a factor of ~2, the temperatures would be <10 and ~30 K for α- and β-$c(2\times2)$, respectively.

VI. CONCLUSIONS

We found two types of Mn/Pd(001) surface alloys and determined these structures by the LEED analysis. At lower coverages the surface consists of a Pd first layer and a Pd-Mn mixed second layer, and at higher coverages the surface consists of Pd-Mn mixed first and third layers and a Pd second layer. Both surfaces are similar to the different types of terminations of the bulk MnPd$_3$ alloy of the AuCu$_3$ type. We also studied the magnetic property of these surfaces by MOKE measurement. No magnetic responses were observed at 10 K. The total-energy calculation suggests that the Mn atoms in these surface alloys keep large magnetic moments, but the exchange integrals are too small to establish long-range magnetic order.

*Email address: aruga@kuchem.kyoto-u.ac.jp

[1] *A Handbook of Lattice Spacings and Structures of Metals and Alloys*, edited by W. B. Pearson (Pergamon Press, New York 1958).

[2] *Magnetic Materials*, edited by R. S. Tebble and D. J. Craik (Wiley-Interscience, New York 1969).

[3] D. Tian, R. F. Lin, F. Jona, and P. M. Marcus, Solid State Commun. **74**, 1017 (1990).

[4] D. Tian, S. C. Wu, F. Jona, and P. M. Marcus, Solid State Commun. **70**, 199 (1989).

[5] M. Wuttig, Y. Gauthier, and S. Blügel, Phys. Rev. Lett. **70**, 3619 (1993).

[6] M. Wuttig, C. C. Knight, T. Flores, and Y. Gauthier, Surf. Sci. **292**, 189 (1993).

[7] Wondong Kim, Wookje Kim, S.-J. Oh, J. Seo, J.-S. Kim, H.-G. Min, and S.-C. Hong, Phys. Rev. B **57**, 8823 (1998).

[8] Wondong Kim, S.-J. Oh, Jikeun Seo, H. G. Min, S. C. Hong, and J.-S. Kim, Phys. Rev. B **65**, 205407 (2002).

[9] P. Schieffer, C. Krembel, M.-C. Hanf, G. Gewinner, and Y. Gauthier, Phys. Rev. B **62**, 2944 (2000).

[10] W. L. O'Brien and B. P. Tonner, J. Appl. Phys. **76**, 6468 (1994).

[11] N. W. Ashcroft and N. D. Memin, *Solid State Physics* (Saunders College Publishing, Philadelphia, 1976).

[12] V. S. Stepanyuk, W. Hergert, K. Wildberger, R. Zeller, and P. H. Dederichs, Phys. Rev. B **53**, 2121 (1996).

[13] S. Blügel, M. Weinert, and P. H. Dederichs, Phys. Rev. Lett. **60**, 1077 (1988).

[14] J. M. Khalifeh and B. A. Hamad, Physica B **321**, 230 (2002).

[15] A. J. Jaworowski, S. M. Gray, M. Evans, R. Asmundsson, P. Uvdal, and A. Sandell, Phys. Rev. B **63**, 125401 (2001).

[16] A. Sandell, P. H. Andersson, E. Holmström, A. J. Jaworowski, and L. Nordström, Phys. Rev. B **65**, 035410 (2001).

[17] A. Barbieri and M. A. Van Hove, SYMMETRIZED AUTOMATED TENSOR LEED package, available from M. A. Van Hove; http://electron.lbl.gov/vanhove/vanhove.html.

[18] *Surface Crystallography by LEED*, edited by M. A. Van Hove and S. Y. Tong (Springer-Verlag, Berlin 1979).

[19] J. B. Pendry, J. Phys. C **13**, 937 (1980).

[20] P. Blaha, K. Schwarz, G. K. H. Madsen, K. Kvasnicka, and J. Luitz, WIEN2k, *An Augmented Plane Wave + Local Orbital Program for Calculating Crystal Properties* (Technical Universitat Wien, Wien, Austria, 2001).

[21] K. Schwarz, P. Blaha, and G. K. H. Madsen, Comput. Phys. Commun. **147**, 71 (2001).

[22] E. Sjöstedt, L. Nordström, and D. J. Singh, Solid State Commun. **114**, 15 (2000).

[23] G. K. H. Madsen, P. Blaha, K. Schwarz, E. Sjöstedt, and L. Nordström, Phys. Rev. B **64**, 195134 (2001).

[24] J. P. Perdew, K. Burke, and M. Ernzerhof, Phys. Rev. Lett. **77**, 3865 (1996).

[25] Per Önnerud, Yvonne Andersson, and Roland Tellgren, J. Solid State Chem. **128**, 109 (1997).

[26] E. Krén and G. Kádár, Phys. Lett. A **29A**, 340 (1969).

[27] J. W. Cable, E. O. Wollan, W. C. Koehler, and H. R. Child, Phys. Rev. **128**, 2118 (1962).

[28] N. Tsuboi, H. Okuyama, M. Nishijima, and T. Aruga, Phys. Rev. B **68**, 033408 (2003).

[29] N. Tsuboi, H. Okuyama, M. Nishijima, and T. Arug (unpublished).

[30] V. L. Moruzzi, P. M. Marcus, and P. C. Pattnaik, Phys. Rev. B **37**, 8003 (1988).